Accepted Manuscript

Full Length Article

Tailoring properties of reduced graphene oxide by oxygen plasma treatment

Izabela Kondratowicz, Małgorzata Nadolska, Samet Şahin, Marcin Łapiński, Marta Prześniak-Welenc, Mirosław Sawczak, Eileen H. Yu, Wojciech Sadowski, Kamila Żelechowska

Please cite this article as: I. Kondratowicz, M. Nadolska, S. Şahin, M. Łapiński, M. Prześniak-Welenc, M. Sawczak, E.H. Yu, W. Sadowski, K. Żelechowska, Tailoring properties of reduced graphene oxide by oxygen plasma treatment, *Applied Surface Science* (2018), doi: https://doi.org/10.1016/j.apsusc.2018.01.168

Tailoring properties of reduced graphene oxide by oxygen plasma treatment

Izabela Kondratowicz[a,3], Małgorzata Nadolska[a,3], Samet Şahin[b,2], Marcin Łapiński[a], Marta Prześniak-Welenc[a], Mirosław Sawczak[c], Eileen H. Yu[b], Wojciech Sadowski[a], Kamila Żelechowska[a,1]

[a]*Faculty of Applied Physics and Mathematics, Gdansk University of Technology, Narutowicza St. 11/12; 80-233 Gdansk, Poland*

[b]*School of Chemical Engineering and Advanced Materials, Merz Court, Newcastle University, Newcastle upon Tyne, UK*

[c]*Centre for Plasma and Laser Engineering, The Szewalski Institute of Fluid Flow Machinery, Polish Academy of Science, Fiszera 14, Gdansk 80-231, Poland*

Abstract

We report an easily controllable, eco-friendly method for tailoring the properties of reduced graphene oxide (rGO) by means of oxygen plasma. The effect of oxygen plasma treatment time (1, 5 and 10 minutes) on the surface properties of rGO was evaluated. Physicochemical characterization using microscopic, spectroscopic and thermal techniques was performed. The results revealed that different oxygen-containing groups (e.g. carboxyl, hydroxyl) were introduced on the rGO surface enhancing its wettability. Furthermore, upon longer treatment time, other functionalities were created (e.g. quinones, lactones). Moreover, external surface of rGO was partially etched resulting in an increase of the material surface area and porosity. Finally, the oxygen plasma-treated rGO electrodes with bilirubin oxidase were tested for oxygen reduction reaction. The study showed that rGO treated for 10 min exhibited twofold higher current density than untreated rGO. The oxygen plasma treatment may improve the enzyme adsorption on rGO electrodes by introduction of oxygen moieties and increasing the porosity.

[1]Corresponding author. Tel: +48 58 348 66 16.
E-mail address: kzelechowska@mif.pg.gda.pl (K. Zelechowska)
[2]Permanent address: Department of Chemical and Process Engineering, Faculty of Engineering, Bilecik Şeyh, Edebali University, Bilecik, Turkey
[3]Both authors contributed equally to this work

1. Introduction

Graphene-based structures are among the most promising materials for various applications due to the high surface area and good electrical conductivity. Reduced graphene oxide (rGO), one of the derivatives of graphene, is widely used due to its low-cost and scalable production [1-8]. However, the main limitations to the development of rGO are its weak chemical reactivity and poor wettability due to its hydrophobic nature after oxygen group removal. Therefore, different methods that are mainly chemical have been employed to functionalize rGO surface [9-11]. The use of harsh chemicals and the release of toxic gases during such synthesis make these methods harmful for the environment, hard to control and time consuming. Furthermore, some amounts of material (about 20-30%) are usually lost during the washing process. Therefore, safe, controllable, eco-friendly and simple methods to introduce oxygen groups to rGO are demanded.

Oxygen plasma treatment of carbonaceous materials is another commonly used approach. Compared to chemical methods, this method is environmentally benign and safe, only needs few minutes of reaction time, as well as causes a negligible loss of a material. The O_2 plasma provides a way to conveniently introduce the surface oxygen functionalities by reaction of atomic oxygen species with carbon atoms. Two effects from these interactions are expected: the removal of outermost carbon atoms by etching reactions, and/or the introduction of new oxygen-containing chemical groups. For both cases, only the external surface of carbon material is modified [12-14].

There are few papers focusing on the O_2 plasma treatment of different carbon-based materials [15-19]. Tascon *et al.* [15] modified the surface of carbon fibres using O_2 plasma introducing oxygen functionalities on the surface. Haji *et al.* [16] found that the surface roughness as well as the concentration of reactive functional groups on the carbon fibre surface was increased after plasma treatment. Sanada *et al.* [17] modified the surface of carbon black and showed that mainly O-C-O, C=O and O-C=O groups were introduced after O_2 plasma exposure. However, the use of O_2 plasma in the treatment of novel carbon nanomaterials is still limited. To the best of our knowledge, there are only few reports showing the effect of O_2 plasma on graphene, carbon nanotubes and rGO [20-23]. Mulher *et al.* [20] treated multiwalled carbon nanotubes with nitric acid and O_2 plasma. The acid treatment introduced mainly carboxylic and phenolic groups, whereas plasma functionalization caused the grafting of C=O groups. Favia *et al.* [21] recently demonstrated an efficient method to modify carbon nanotubes by O_2 plasma in order to improve their aqueous dispersions. More recently, Hwang *et al.* [22] modified chemically reduced GO with O_2 plasma and managed to improve its surface reactivity for biomolecular interactions. Despite the above studies, a full understanding of the influence of O_2 plasma treatment on the surface chemistry of rGO is still lacking.

In this work, we used low-pressure oxygen plasma for rGO functionalization. The effect of O_2 plasma treatment time (i.e. 1, 5 and 10 minutes) on the surface chemistry of rGO was systematically analysed

by infrared spectroscopy (FTIR), X-ray photoelectron spectroscopy (XPS) and thermogravimetry (TG). A new metric was applied for the analysis of Raman spectra. The morphology was analysed by scanning electron microscope (SEM). Brunauer-Emmett-Teller (BET) method was used to detect variations in the surface areas of samples. Finally, the adsorption of bilirubin oxidase (BOD) on rGO samples was performed and electrochemical characterisation of the prepared samples was studied using cyclic voltammetry (CV) to compare the activities of rGO-enzyme electrodes towards oxygen reduction reaction (ORR). It was demonstrated that the surface chemistry of rGO strongly depends on the treatment time which results in an introduction of different oxygen-containing functionalities and an increase in the surface roughness and porosity.

2. Experimental

2.1. *Materials and reagents*

Ammonia (25%) was purchased from POCh (Gliwice, Poland). N-Methyl-2-pyrrolidone (NMP) were purchased from Chempur, Poland. Hydrazine monohydrate, BOD from Myrothecium verrucaria (lyophilized powder, 15-65 units/mg protein) were purchased from Sigma-Aldrich.

2.2. *Synthesis of reduced graphene oxide powders*

GO was obtained by improved Hummers' method which was described in our previous reports [24-26]. Ball-milling technique was applied herein in order to obtain smaller, more reactive GO flakes (See Supporting Info). The rGO powders were synthesized by chemical reduction of GO followed by thermal reduction. 200 μL of hydrazine hydrate was added to 200 mL of GO aqueous dispersion (1 mg/mL) and pH was adjusted to 10 with the addition of ammonia (25%). Dispersion was heated up to 90°C in an oil bath and stirred magnetically for 7 hours. The sample was then centrifuged at 15000 rpm for 10 min and washed thoroughly with deionized water. The powder was further reduced thermally at 600°C for 5 h in an argon atmosphere.

2.3. *Preparation of O_2 plasma-treated rGO*

The oxygen plasma functionalization of rGO was carried out in a Femto low-pressure plasma reactor with the 13.56 MHz RF power generator (Diener Electronic). The rGO powder was divided into four samples (of 50 mg each) and placed evenly at the bottom of Pyrex vials to ensure the full contact with plasma. The RF input power (50 W) and oxygen flow rate (10 sccm) were kept constant while the effect of treatment time (1, 5 and 10 minutes) was studied. Untreated sample was denoted as **rGO**. Samples treated with plasma with different time intervals were denoted as **rGO-1min, rGO-5min** and **rGO-10min**.

2.4. Characterization techniques

The morphology of the samples was analyzed with a scanning electron microscopy (ESEM Quanta Feg 250, FEI). Raman spectra were recorded using a Renishaw InVia spectroscope with argon ion laser operating at 514.5 nm focused through a 50x objective. The collected light was dispersed through a triple monochromator and detected with a charge coupled device. A total of 3 acquisitions were recorded for each sample. The spectra were collected in the dark, with a resolution of 2 cm^{-1} in the range of 100–3200 cm^{-1}. BET surface area was determined using Gemini V Micrometrics pore and surface analyser (Micrometrics Instrument Corporation, U.S.A) in the relative pressure range (p/p$_0$) 0.05–0.3. Before measurement, samples were degassed in N_2 at 200 °C for 2 h. The adsorption analysis was performed at 77 K. The total pore volume was determined via Barret-Joyner-Halenda (BJH) method.The FTIR spectra were recorded using the KBr pellet method on a Perkin Elmer Frontier spectrophotometer with resolution of 2 cm^{-1} in the range of 500–4000 cm^{-1}. XPS analyses were carried out with X-ray photoelectron spectrometer (Omicron NanoTechnology) with 128-channel collector. The measurements were performed with constant energy mode (CAE) with energy pass equal to 50 eV at room temperature in a ultra-high vacuum conditions, below $1.1 \cdot 10^{-8}$ mbar. The photoelectrons were excited by an Mg-Kα X-Ray source. The X-ray anode was operated at 15 keV and 300 W. Omicron Argus hemispherical electron analyser with round aperture of 4 mm and pass energy of 50 eV was used for analysing of emitted photoelectrons. The binding energies were corrected using the background C1s line corresponding to C=C bonds (285.0 eV) as a reference. [27] Samples were pressed into pellets of c.a. 6 mm diameter in order to ensure their homogeneity. XPS spectra were recorded using a small 0.03 eV step size, scanning a sample area of about 2mm x 2mm. XPS spectra were analysed with Casa-XPS software using a Shirley background subtraction and least-square Gaussian–Lorentzian curve as a fitting algorithm. TGA was performed under synthetic air with heating rate 5°C/min from 40°C to 900°C using Netzsch STA 449 F1. The STA449 F1 has a vertical sample carrier and in order to account for buoyancy effects, a correction curve with empty crucibles was first obtained and then subtracted from the experimental results. To avoid heat and mass transfer limitations, approximately 8 mg of sample was used, and Al_2O_3 crucibles with lids were employed. The total uncertainty associated with measurement was 0.005% by weight of the sample and was included in the final result.

2.5. Fabrication and electrochemical characterization of enzymatic electrodes

Screen-printed carbon electrode (SPE, model DRP-C110, WE diameter of 0.40 cm and a surface area of 0.126 cm^2) was purchased from DropSens (Oviedo, Spain). The reference electrode for carbon SPEs is silver/silver ion (Ag/Ag$^+$, 0.74 V *vs* SHE) and the counter electrode is carbon. The electrodes were stored at room temperature in a dry place and no pre-treatment was applied.

To prepare enzymatic rGO electrodes, 2 μL of rGO dispersion in H_2O/NMP (0.5 mg/mL, 50:50 v/v %) was drop casted onto SPE and dried at room temperature. The dispersion was sonicated for at least 10 minutes before each drop casting to provide uniform coating on SPEs. 20 μL of BOD (4 mg/mL in 0.1 M phosphate buffer solution (PBS), pH=7) was then applied on electrode surface for adsorption overnight at 4 °C. Electrodes were rinsed with 0.1 M PBS at pH 7 to remove weakly adsorbed enzyme before use and tested without further treatment. CV was applied to the electrodes placed in a perspex cell containing 0.1 M PBS solution at at pH 7 saturated with either nitrogen or air. Nitrogen or air blanket was maintained throughout the experiments.

3. Results and discussion

3.1. *Morphology and surface area characterization of rGO samples treated with oxygen plasma*

Untreated rGO and O_2 plasma-treated samples were dispersed in water (5 mL, 1 mg/mL) and sonicated for 10 min. ~~Figure 1 shows a digital picture of the dispersions.~~ This measurements were conducted on the fifth day after the plasma treatment. A digital picture of dispersions taken immediately after sonication is presented in Figure 1. The first visual observations confirm the introduction of different amount of oxygen functionalities on rGO surface. ~~Immediate~~ Prompt precipitation was observed for untreated rGO sample after few minutes of sonication, while rGO-1min and rGO-5min dispersions became black with no noticeable precipitation. Moreover, dispersion of rGO-10min showed more precipitation in comparison to samples prepared after 1 and 5 minutes of plasma treatment. This may suggest that different types of oxygen functionalities with varying degrees were introduced in this sample. In order to evaluate the stability, the resulting dispersions were observed over time. Figure S1 shows water-dispersed samples, after 3 and 7 days from the preparation, respectively. All of O_2-treated samples revealed the deterioration of hydrophilicity with time. Such an effect is connected with sample aging and is commonly observed for plasma treated carbon-based materials [28-30]. However, it should be noticed that even after a week, aqueous dispersions of treated samples are more stable than of untreated rGO.
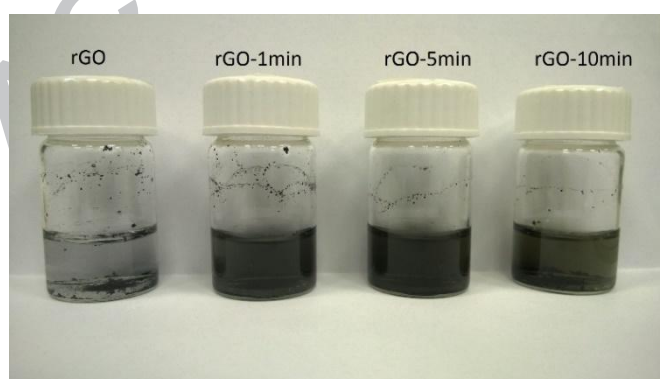

Figure 1: Aqueous dispersions of untreated rGO, and O_2-plasma treated rGO-1min, rGO-5min and rGO-10min.

The morphological changes of rGO samples were investigated using SEM. Images of untreated rGO, rGO-1min, rGO-5min and rGO-10min are shown in Figure 2. The SEM image of rGO (Fig. 2a) clearly exhibits a layered structure with wrinkled graphene sheets. No noticeable porosity is observed in this sample. After O_2 plasma treatment, the surface of rGO become more porous and corrugated (Figure 2b-d). It can be seen that graphene sheets are more aggregated with rougher and porous surface. Surface of rGO-10min is also highly porous and partially damaged. The inner graphene layers can be observed in this sample, which may be revealed after plasma etching.
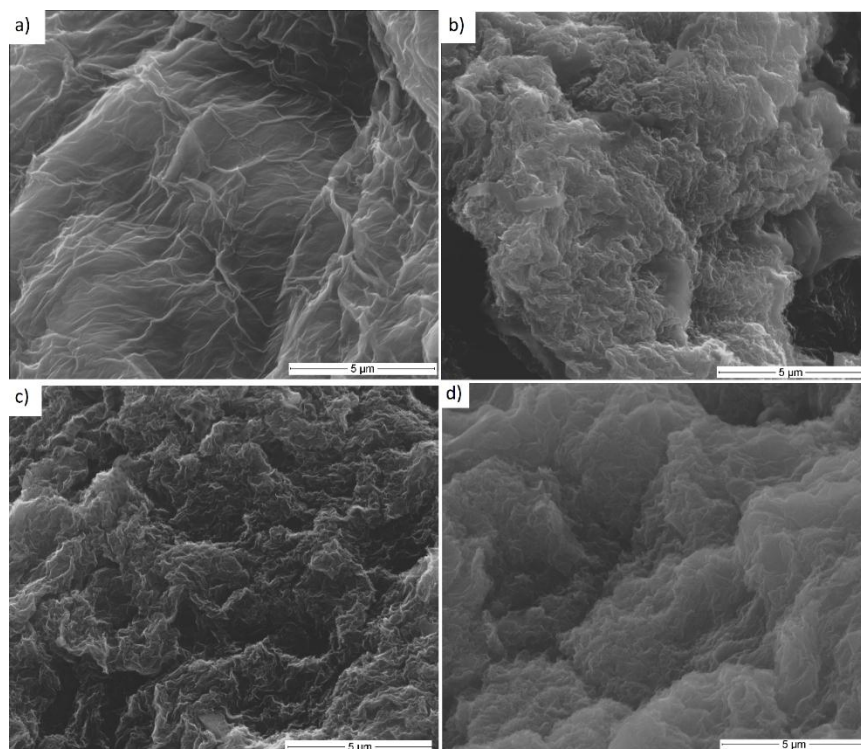

Figure 2: SEM images of a) rGO, b) rGO-1min, c) rGO-5min and d) rGO-10min samples.

The specific surface areas of rGO samples were evaluated by the BET method. The results are shown in Table 1. BET surface area of untreated rGO was found to be only about 30 m^2/g and increased to 250 m^2/g for rGO-10min. Total pore volume increased from 0.014 cm^3/g for rGO to 0.123 for rGO-10min. These significant changes suggest that the oxygen species in plasma may cause the surface etching as well as pore opening in the samples resulting in an increase in the specific surface area and total pore volume.

Table 1: BET surface area and total pore volume of untreated rGO and O_2 plasma treated rGO samples.

Sample	rGO	rGO-1min	rGO-5min	rGO-10min
BET surface area (m^2/g)	29.8	93.5	222.1	249.1
Total pore volume	0.014	0.047	0.110	0.123

(cm^3/g)

3.2. Surface chemistry change after oxygen plasma treatment of rGO

In this study, a new Raman metric for the investigation of rGO was used, based on the method suggested by King *et al.* [28]. According to this method, the experimental Raman spectra were deconvoluted into five Lorentzian components giving rise to six peaks in total namely D, G, apparent G_{app}, D', 2D and 2D' placed at about 1350, 1580, 1590, 1610, 2690 and 2950 cm^{-1}, respectively, and varying for different O$_2$ plasma-treated rGO samples (Figure 3). The D band due to the first order scattering of A1g mode and its overtone, 2D band, due to the second order scattering of A1g mode are typical features for defective graphene derivatives. Formation of sp^3 carbon bonds and other structural defects results in an appearance of these bands. The 2D peak in GO and rGO spectra is often accompanied by higher order peak 2D', an overtone of D' mode. The typical G band due to the first order scattering of the E2g mode is observed in all graphene-like samples [22, 29]. This band, named here as apparent G_{app} is, however, a superposition of G and D' modes, which is very often neglected in the literature. King *et al.* [28] suggest that the position difference between D' and G_{app} is one of the main parameters that should be taken into consideration when comparing GO and rGO samples. Table 2 presents D'-G_{app} values of all samples along with other parameters that can help understand the differences between GO and rGO through the analysis of the Raman spectra.
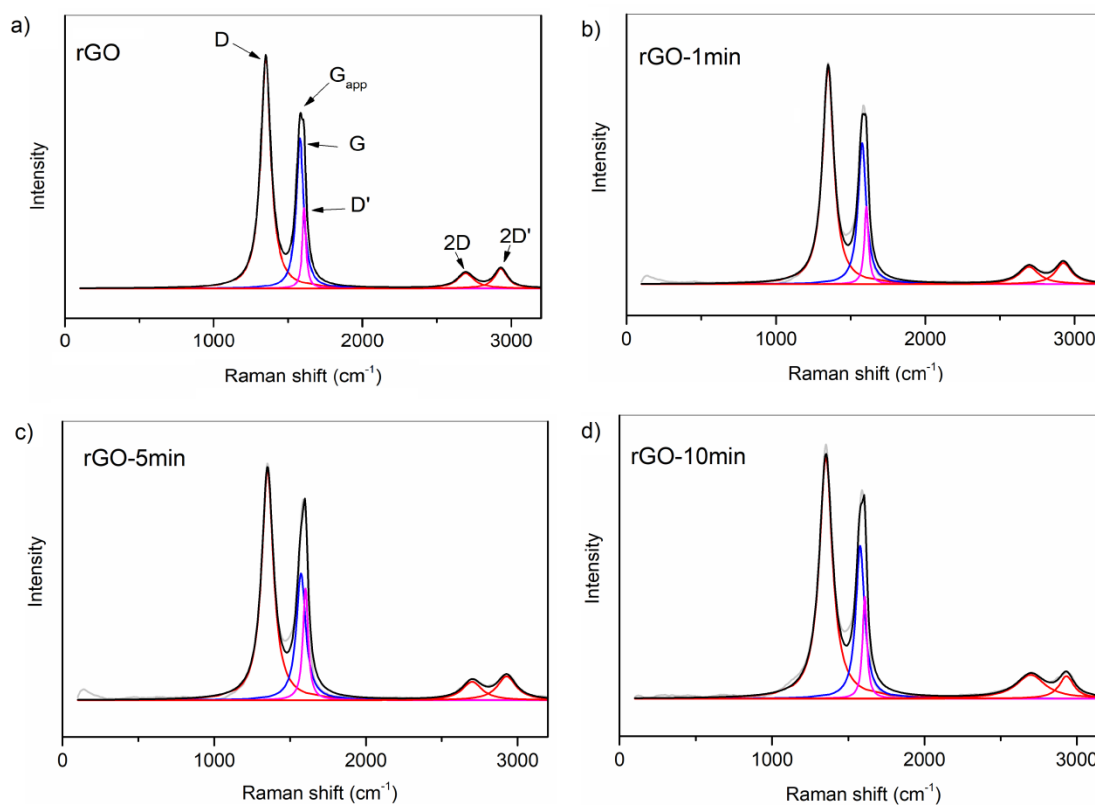
Figure 3: Raman spectra of a) untreated rGO, b) rGO-1min, c) rGO-5min and d) rGO-10min.

King *et al.* [28] suggested that when the D'-G_{app} value ranges between 0 and 25, material can be defined as rGO whereas below and above this limit GO and pure graphene can be defined, respectively. This is in accordance with our results in which D'-G_{app} value decreased from 20.1 for untreated rGO to 14.2 for rGO-5min which can be attributed to more oxygen-containing groups or defects on the surface. Unexpectedly, for rGO-10min sample an increase in D'-G_{app} is observed, comparing to rGO-5min. Furthermore, the position of the G band increased for rGO-10min. These results can be explained as follows. As shown before in SEM images, after 10 min of O_2 plasma exposure, the surface of rGO was slightly etched and became rough and porous, which was also observed for other carbon materials [17]. Therefore, we suggest that it may not only be the outer surface of the rGO that is observed and analyzed, but also the underlying, inner sheets of rGO. Furthermore, full width at half maximum (FWHM) of D band is often considered as a measure of defect sites on the surface. FWHM of D band increased from 83.0 cm^{-1} for untreated rGO to 96.9 cm^{-1} for rGO-10min which suggests the most defective structure of the latter. A number of studies [29-31] showed that I_D/I_G ratio (which is in fact a I_D/I_{Gapp} ratio, according to the new metric) can be used to compare GO and rGO. However, due to the superposition of G_{app} band, I_D/I_{Gapp} ratio is no longer relevant. Instead, I_{2D}/I_G ratio can be taken into account, as a measure of the defects concentration. For O_2 plasma-treated samples, I_{2D}/I_G ratio increased from 0.23 for untreated rGO to 0.93 for rGO-10min. These results showed that by increasing the plasma treatment time, more defective structure of rGO is obtained.

Table 2: Different parameters, as analyzed from deconvoluted Raman peaks for rGO, rGO-1min, rGO-5min, rGO-10min

Samples	D'-G_{app} (cm^{-1})	D FWHM (cm^{-1})	D' FWHM (cm^{-1})	G position (cm^{-1})	I_{2D}/I_G
rGO	20.1	83.0	30.1	1579.1	0.23
rGO-1min	18.6	90.5	32.4	1576.3	0.28
rGO-5min	14.2	93.0	40.7	1572.2	0.35
rGO-10min	17.9	96.9	69.3	1577.8	0.93

Figure 4 shows the FTIR spectra of untreated rGO and O_2 plasma-treated rGO samples. Several distinct bands can be observed in all rGO samples. Wide, broad bands with the maximum at 3440 cm^{-1} can be ascribed to -OH bonding from hydroxyl groups (such as phenolic, carboxyl) and water molecules. Small band at about 1640 cm^{-1} can be ascribed to C=O carbonyl group that can be present in carboxylic and/or quinone functional groups. A sharp band at about 1560 cm^{-1} can be associated to

the stretching vibrations of double C=C bonds conjugated with C-C/C=O bonds. A broad band ranging from 1180 to 1040 cm^{-1} can be ascribed to C-O bonds in carboxyls, epoxy groups and alcoxyls. It can be seen that additional bands appeared at the spectra of O$_2$ plasma-treated samples. A new band at around 1730 cm^{-1} can be observed in rGO-5min and rGO-10min which confirms the presence of C=O groups from lactones. In the spectrum of rGO-10min, an additional band at 1436 cm^{-1} appeared which can be associated with C-O lactone groups.
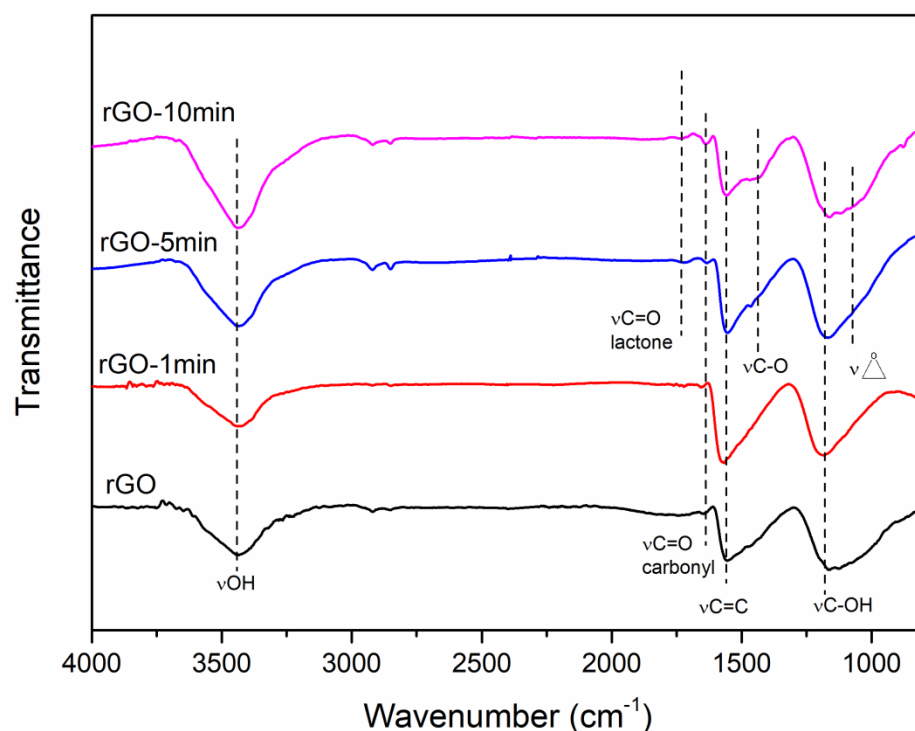

Figure 4: FTIR spectra of untreated rGO and O$_2$ plasma-treated rGO-1min, rGO-5min and rGO-10min samples.

The presence of oxygen-containing functionalities was further confirmed by XPS method. The C1s and O1s peaks for all samples were observed at about 285 and 533 eV, respectively. The surface atomic content was determined from the analysis of areas under C1s and O1s survey spectra, taking into account the atomic sensitivity factors. Table 3 shows the atomic contents (at%) of C and O, along with the C:O atomic ratio. The untreated rGO sample exhibited the oxygen content of about 23.2 at% and C:O ratio of 3.3, which is in agreement with other literature data [5, 32]. After O$_2$ plasma treatment, the oxygen content increased, as expected. The rGO-1min and rGO-10min samples showed the highest oxygen content (31.0% and 26.7%, respectively) and the lowest C:O ratio (2.2 and 2.8, respectively).

Table 3: Surface atomic content (at%) of C and O for all rGO samples.

Sample	Atomic content (at%)		
	C	O	C:O

rGO	76.8±0.3	23.2±0.1	3.3±0.1
rGO-1min	69.0±0.2	31.0±0.2	2.2±0.1
rGO-5min	75.3±0.2	24.7±0.1	3.1±0.1
rGO-10min	73.3±0.3	26.7±0.1	2.8±0.1

High resolution XPS spectra with curve fittings for C1s range of all samples are shown in Figure 5. The binding energies were corrected by setting the C=C/C-C bonds peak at 285.0 eV in all spectra. In untreated rGO spectrum (Fig. 5a) two distinct peaks can be found at 286.4 eV (C-O groups) and at 289.0 eV (carboxyl C(O)O groups). For O_2 plasma-treated samples (Fig. 5b-d), in addition to C-O and C(O)O peaks, a new peak at about 287.6 eV can be observed and assigned to C=O groups.
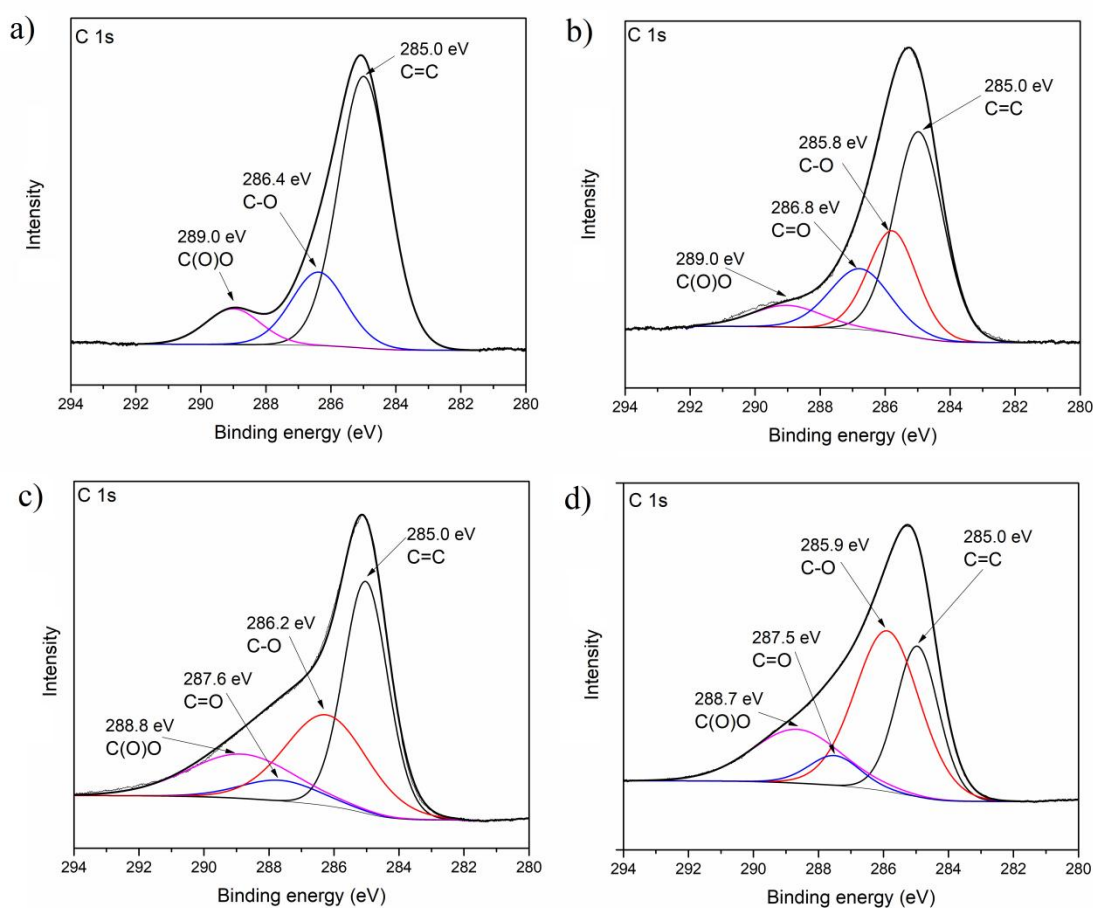

Figure 5: The XPS spectra related to C1s electrons of a) rGO, b) rGO-1min, c) rGO-5min and d) rGO-10min. In all spectra the continuous black lines are the optimum fit of the experimental data and grey lines are different components obtained by deconvolution.

By the analysis of the area under all deconvoluted curves, the atomic content of C and O functional groups was evaluated. Figure 6 shows the atomic content of C and O functional groups as a function of O_2 plasma treatment time.
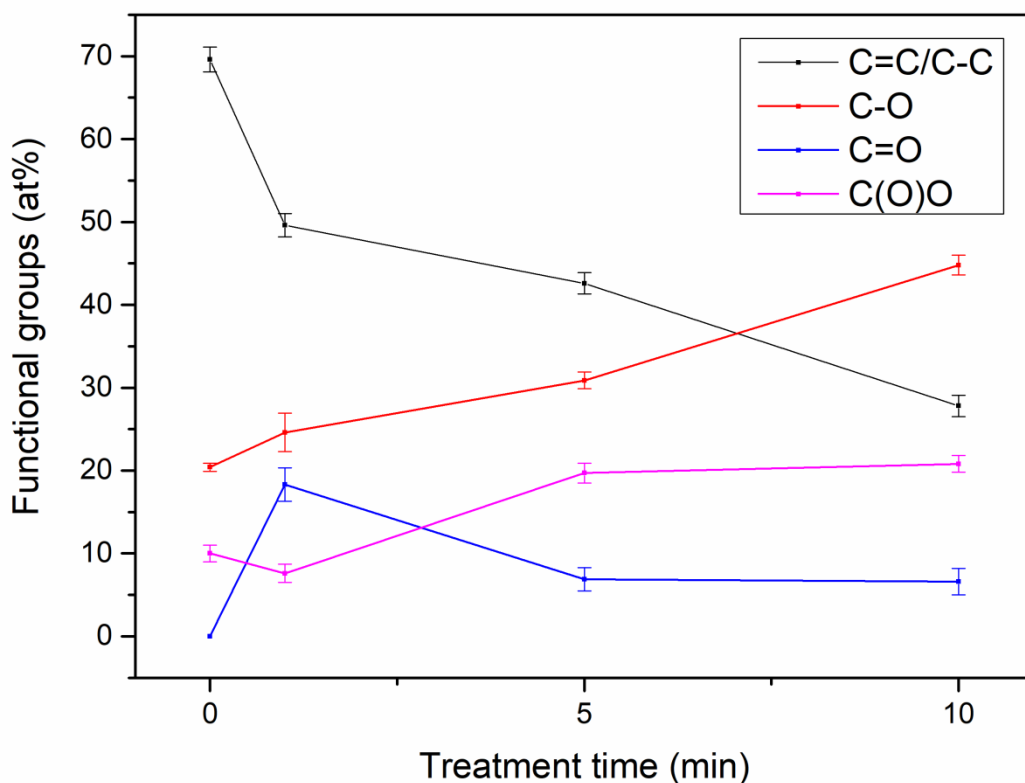
Figure 6: Atomic content of C- and O-functional groups as a function of O_2 plasma treatment time. Black solid lines are given only as guides to the eye.

It can be seen that the content of C=C/C-C groups decreased after O_2 plasma treatment from about 70 at% for untreated rGO to 28 at% for rGO-10min. This may indicate that the carbon-carbon network was disrupted after O_2 plasma treatment. The results also show that the content of C-O (epoxy, hydroxyl) groups increased for rGO-10min comparing to untreated rGO. Interestingly, the highest amount of C=O (carbonyl and quinone) bonds can be found in rGO-1min sample and further decreased for rGO-5min and rGO-10min samples. This phenomenon can be explained by analyzing the influence of O_2 plasma on the surface of rGO. It is known that O_2 plasma contains positive and negative ions, electrons and emits UV that have enough energy to break chemical bonds at the external surface of a material. Different radicals can be therefore created by reaction with oxygen and produce various oxygen-containing polar groups, such as OH, COOH, C-O, C=O, etc. These groups can be observed in rGO and rGO-1min samples. According to the well-known reactions, phenol/catechol groups that are placed on the edges of the rGO sheets can be further converted into quinone groups (denoted as '1' in Figure 7). After longer exposure to O_2 plasma (5-10 minutes), carboxyl groups that are placed in the vicinity of hydroxyl groups can merge and create lactone groups (See '2' in Figure 7). During the creation of lactones, one oxygen atom is lost due to the formation of water molecule, therefore the atomic content of oxygen in these samples should decrease. This is in agreement with the results shown in Table 3. The atomic content of C=O (carbonyl/quinone) groups decreased for rGO-

5min and rGO-10min in comparison to rGO-1min. At the same time, the atomic content of C(O)O (carboxyl/lactone) groups increased for rGO-5min and rGO-10min. This is in accordance with FTIR spectra which showed a new band for C=O lactone groups for rGO-5min and rGO-10min samples. Therefore, we suggest that rGO-1min sample may contain quinone groups that were formed from residual hydroxyl groups present in rGO. Furthermore, after 5 to 10 min of plasma exposure, the formation of quinones may be inhibited, and lactone groups are created in more extent and epoxy groups are introduced. These groups are non-polar which also explains the hydrophobic nature of rGO-10min sample, as shown in Section 3.1.
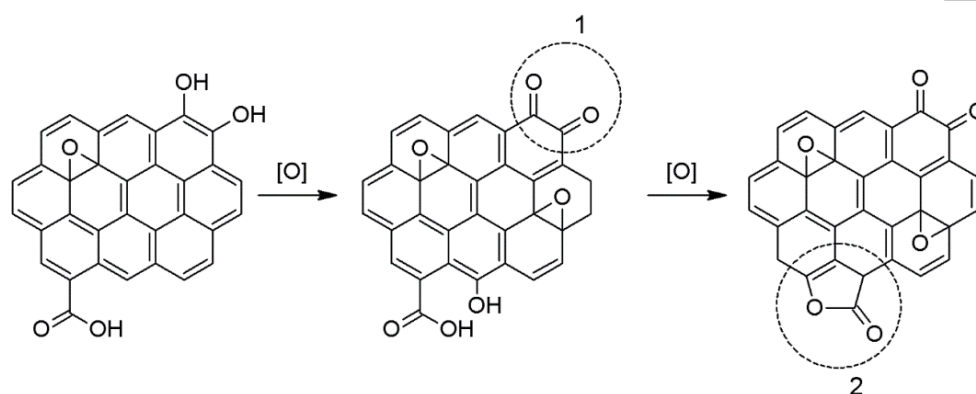

Figure 7: The scheme showing the proposed formation of quinone (1) and lactone (2) groups after O_2 plasma treatment of reduced graphene oxide.

3.3. *Effect of treatment time on degree of surface functionalization*

The degree of surface functionalization before and after O_2 plasma treatment was also determined by TGA. Figure 8 shows the TGA curves that present the mass as a function of temperature. The mass loss (%) in different temperature range is shown in Table 4. Three regions can be distinguished in the spectra which is a characteristic for GO and rGO materials [33-35]. In the first region (up to 150°C), evaporation of adsorbed water molecules occurs which causes a slight mass loss (about 1%) for all samples. In the temperature range of 150-300°C, labile oxygen-containing functional groups are decomposed (such as carboxyl, epoxy, lactone), yielding CO, CO_2 and steam. In this temperature range, untreated rGO exhibits mass loss of about 0.6%. This indicates that untreated rGO still contains some functional groups after GO reduction. The mass loss is slightly higher for O_2 plasma-treated samples (0.8-1.4%) in comparison to rGO. This suggests that additional functionalities were introduced during the plasma treatment. At higher temperatures (III region), the most stable groups (such as carbonyl/quinone) decompose as well as the pyrolysis of carbon skeleton takes place. In this temperature range, noticeable weight loss was observed for rGO-1min and rGO-10min samples (7.6% and 7.3%, respectively), indicating that these samples may have the most disrupted structure due to the introduction of more stable oxygen functionalities. This is in agreement with XPS results showing that rGO-1min sample may contain more carbonyl/quinone groups than other samples. Interestingly, in this

temperature range, the highest weight loss was observed for rGO-1min (7.6%) and rGO-10min (7.3%). It may therefore be concluded that these samples contain more carbonyl/quinone groups than the others, which is in agreement with XPS results. With increasing treatment time (0, 1, 5 and 10 min), a total mass loss at 900°C was equal to 6.6, 9.4, 9.0 and 10.1%, respectively. These values are significantly lower comparing to the thermal degradation of GO (about 40% of mass loss at 900°C [33-35]), indicating that only a small amount of oxygen groups is introduced after the O_2 plasma treatment, maintaining the thermal stability of materials (3.5% difference in mass loss between rGO and rGO-10min). The variations in TGA curves profiles and mass loss of rGO samples further prove that different types of functional groups were introduced during the plasma treatment.
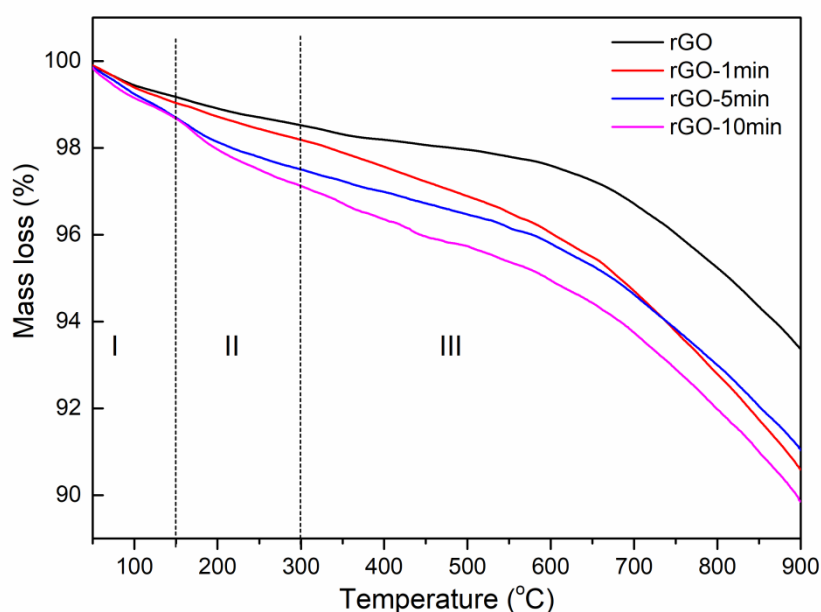

Figure 8: TGA curves of rGO, rGO-1min, rGO-5min and rGO-10min.

Table 4: Mass loss (%) of rGO samples in different temperature ranges.

Temperature range (°C)	Mass loss (%)			
	rGO	rGO-1min	rGO-5min	rGO-10min
40-150	0.8	1.0	1.3	1.3
150-300	0.6	0.8	1.2	1.5
300-900	5.2	7.6	6.5	7.3
40-900	6.6	9.4	9.0	10.1

3.3.1. Electrocatalytic performance of rGO-based enzymatic electrodes

Electrically conductive and porous surface of O_2 plasma-treated rGO can be used in bioelectrochemical applications such as biosensors. The active functional chemical groups introduced by O_2 plasma can be used to adsorb enzymes on the surface. Using this approach, it might be possible

to achieve direct electron transfer (DET) between rGO and the enzyme. In this section, BOD, a multi-copper oxidase, was adsorbed on rGO-coated SPEs and the electrochemical oxygen reduction performance was tested. Figure 9 shows the electrocatalytic response of BOD-modified rGO electrodes to oxygen reduction in phosphate buffer solution (0.1 M PBS, pH=7.0) at a scan rate of 10 mV/s. It can be seen that the onset potential for the enzymatic reduction of oxygen is about 0.25 V (*vs* Ag/Ag$^+$). This is similar to the previously reported values for electrochemical oxygen reduction using BOD in neutral media [36,37]. Table 5 shows the current density values for each electrode calculated after the subtraction of background current from the current obtained in the presence of oxygen in the solution, divided by the area of SPE (0.126 cm^2).
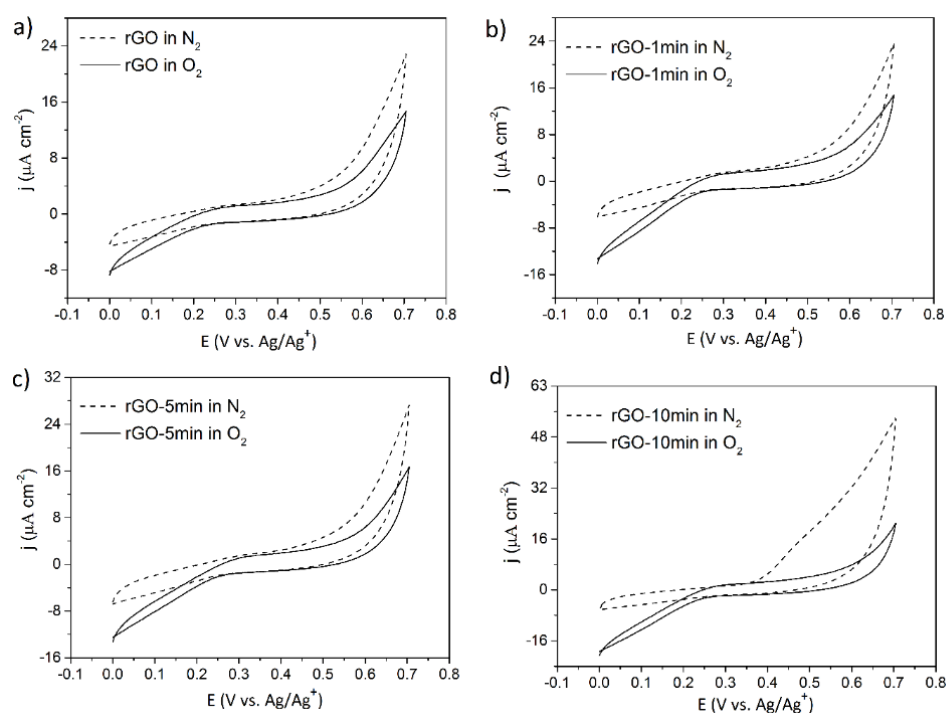

Figure 9: Cyclic voltammograms of a) rGO, b) rGO-1min,c) rGO-5min and d) rGO-10min, tested in nitrogen (dotted line) and oxygen-saturated (solid line) phosphorous buffer solution (pH=7.0) at a scan rate of 10 mV/s.

Table 5 : Current densities at 0 V (in μA/cm^2). All values are calculated after subtraction of the background current (i.e. in the absence of oxygen).

Sample	rGO	rGO-1min	rGO-5min	rGO-10min
Current density (μA/cm^2)	4.8	7.9	5.6	9.9

It can be seen that the rGO-10min electrode showed the highest current density (about 10 μA/cm^2) which is twice as much current as it was obtained for untreated rGO electrode (4.8 μA/cm^2). Interestingly, rGO-1min electrode exhibited higher current density than rGO-5min electrode. According to FTIR, XPS and TGA results shown before, rGO-1min and rGO-10min samples contain

the higher amount of C=O bonds (carbonyl and quinone groups) in comparison to untreated rGO and rGO-5min samples. A number of studies have shown that quinone moieties can facilitate redox reactions [38-40]. Recently, Chen et al. [38] showed that rGO possessing quinone groups can also assist in electron transfer and enhance the enzyme stability and activity. At the same time, more porous and well-developed external surface of rGO-10min electrode may further promote the proper orientation of BOD that helps to achieve efficient DET between enzyme and rGO [41-43]. Therefore, a combination of high amount of carbonyl/quinone groups along with enhanced porosity is a key to improving the electrocatalytic performance of BOD-modified rGO electrodes.

In addition, in our experiment only a small amount of rGO was drop casted on SPE which was limited by the wettability of H_2O/NMP mixture used to prepare the dispersions (e.g. 2 µL of 0.5 mg/mL dispersion, i.e. 1 µg of mass loading). Different mass loading can influence the enzyme adsorption to the surface thus the final performance of electrodes. Therefore the current density per gram (in $A/g \cdot cm^{-2}$) of rGO material should be calculated to have a better comparison with literature data. Table 6 shows the comparison of the electrocatalytic performance of different enzymatic electrodes based on graphene/rGO materials (in $A/g \cdot cm^{-2}$). It can be seen that high value (10 $A/g \cdot cm^{-2}$ for rGO-10min) was obtained in this work suggesting that O_2 plasma processing of rGO can be sufficient for tailoring properties of rGO surface for BOD adsorption.

Table 6: Comparison of the electrocatalytic performance of different enzymatic electrodes based on graphene/rGO materials.

Electrode material	Enzyme	Current density per gram ($A/g \cdot cm^{-2}$)	Reference
Graphene	BOD	0.96	Shiba et al. [44]
Electrochemically reduced GO	BOD deposited/BOD mixed	0.52/9	Tkac et al. [45]
Functionalized rGO	Laccase	9	Cosnier et al. [46]
Small-flakes rGO	BOD	18	Tkac et al. [47]
Oxygen-plasma treated rGO	BOD	10	This work

4. Conclusions

In summary, different oxygen-containing functional groups were introduced on the rGO surface by means of oxygen plasma, as confirmed by spectroscopic studies. BET analysis showed the increase in the specific surface area after plasma treatment. The proposed mechanism of the rGO functionalization by oxygen plasma is as follows. During the first minutes of O_2 plasma exposure, new C-O, C=O, and

COOH and O-H bonds can be formed on rGO surface. After longer treatment time (up to 10 minutes), phenols as well as COOH and OH groups can be further converted into quinone and lactone groups, respectively. Furthermore, the etching of the external surface and pore opening may occur which increased the porosity of rGO. Finally, O_2 plasma-treated rGO samples were used as electrodes for bilirubin oxidase adsorption tested for oxygen reduction activity. The highest current density was obtained by rGO-10min (10 $\mu A/cm^2$). It was found out that O_2 plasma-treated rGO, possessing porous surface with quinone moieties, can be beneficial for efficient adsorption of enzymes for bioelectrochemical applications. O_2 plasma treatment offers a simple and controllable method to tailor the surface properties of rGO. It is clean and reliable, thus may open up future pathways for large-scale applications.

Supporting Information

Experimental details on graphene oxide synthesis and characterization using DLS, CV can be found in Supporting Information.

References

[1] Singh, V.; Joung, D.; Zhai, L.; Das, S.; Khondaker, S. I. and Seal, S. Graphene based materials: Past, present and future. Prog. Mater. Sci., 2011, 56 (8), 1178–1271.

[2] Novoselov, K.S.; Fal'ko, V.I. ; Colombo, L.; Gellert, P.R.; Schwab M.G.; Kim K. A roadmap for graphene, Nature, 2012, 490, 192-200.

[3] Zhu, B. Y. et al. Graphene and Graphene Oxide : Synthesis, Properties and Applications. Adv Mater. 2010, 22 (35), 3906-24.

[4] Gao, W.; Alemany, L. B.; Ci, L.; Ajayan, P. M. New insights into the structure and reduction of graphite oxide. Nat Chem. 2009, 1(5), 403-8.

[5] Morimoto, N.; Kubo, T.; Nishina, Y. Tailoring the Oxygen Content of Graphite and Reduced Graphene Oxide for Specific Applications. Nat. Publ. Gr. 2016, 4–11.

[6] Marcano, D. C. et al. Improved synthesis of graphene oxide. ACS Nano, 2010, 4 (8), 4806–14.

[7] Yu, H. et al. High-efficient Synthesis of Graphene Oxide Based on Improved Hummers Method. Sci. Rep., 2016, 6, 36143.

[8] Chua, C. K.; Pumera, M. Chemical reduction of graphene oxide: a synthetic chemistry viewpoint. Chem. Soc. Rev., 2014, 43 (1), 291–312.

[9] Yazici, E.; Yanik, S.; Yilmaz, M. B. Graphene Oxide Nano-Domain Formation via Wet Chemical Oxidation of Graphene. Carbon, 2017, 111, 822–827.

[10] Xu, X.; Zhou, J.; Jestin, J.; Colombo, V.; Lubineau, G. Preparation of water-soluble graphene nanoplatelets and highly conductive films, Carbon, 2017, 124, 133-141.

[11] Shin, D. G.; Yeo, H.; Ku, B.-C.; Goh, M.; You, N.-H. A Facile Synthesis Method for Highly Water-Dispersible Reduced Graphene Oxide Based on Covalently Linked Pyridinium Salt. Carbon, 2017, 121, 17–24.

[12] Dey, A.; Chroneos, A.; Braithwaite, N. S. J.; Gandhiraman, R. P.; Krishnamurthy, S. Plasma Engineering of Graphene. Appl. Phys. Rev. 2016, 3 (2) no. 021301

[13] Li, X; Horita, K. Electrochemical characterization of carbon black subjected to oxygen plasma. Carbon, 2000, 38 (2),133-8.

[14] Junkar, I.; Hauptman, N.; Rener-Sitar, K.; Klanjšek-Gunde, M.; Cvelbar, U. Surface Modification of Graphite by Oxygen Plasma. Inf. MIDEM 2008, 38 (4), 266–271.

[15] Boudou, J. P.; Paredes, J. I.; Cuesta, A.; Martínez-Alonso, A.; Tascón, J. M. D. Oxygen Plasma Modification of Pitch-Based Isotropic Carbon Fibres. Carbon, 2003, 41 (1), 41–56.

[16] Baghery Borooj, M.; Mousavi Shoushtari, A.; Nosratian Sabet, E.; Haji, A. Influence of Oxygen Plasma Treatment Parameters on the Properties of Carbon Fiber. J. Adhes. Sci. Technol. 2016, 2372-82.

[17] Takada, T.; Nakahara, M.; Kumagai, H.; Sanada, Y. Surface Modification and Characterization of Carbon Black With Oxygen Plasma. Carbon, 1996, 34 [9], 1087–91.

[18] Wang, Z.; Yang, F. H.; Yang, R. T. Enhanced Hydrogen Spillover on Carbon Surfaces Modified by Oxygen Plasma. J. Phys. Chem. C 2010, 114 [3], 1601–09.

[19] Rost, U. Effect of Process Parameters for Oxygen Plasma Activation of Carbon Nanofibers on the Characteristics of Deposited Platinum Nanoparticles as Electrocatalyst in Proton Exchange Membrane Fuel Cells. Int. J. Electrochem. Sci. 2016, 11, 9110–22.

[20] Xia, W.; Wang, Y.; Bergsträßer, R.; Kundu, S.; Muhler, M. Surface Characterization of Oxygen-Functionalized Multi-Walled Carbon Nanotubes by High-Resolution X-Ray Photoelectron Spectroscopy and Temperature-Programmed Desorption. Appl. Surf. Sci. 2007, 254, 247–250.

[21] Garzia Trulli, M.; Sardella, E.; Palumbo, F.; Palazzo, G.; Giannossa, L. C.; Mangone, A.; Comparelli, R.; Musso, S.; Favia, P. Towards Highly Stable Aqueous Dispersions of Multi-Walled Carbon Nanotubes: The Effect of Oxygen Plasma Functionalization. J. Colloid Interface Sci. 2017, 491, 255–264.

[22] Chae, M.-S.; Kim, J.; Jeong, D.; Kim, Y.; Roh, J. H.; Lee, S. M.; Heo, Y.; Kang, J. Y.; Lee, J. H.; Yoon, D. S.; Kim, T. G.; Chang, S. T.; Hwang, K. S. Enhancing Surface Functionality of Reduced Graphene Oxide Biosensors by Oxygen Plasma Treatment for Alzheimer's Disease Diagnosis. Biosens. Bioelectron. 2016, 4 [6], 31–38.

[23] Cheng, H. E.; Wang, Y. Y.; Wu, P. C.; Huang, C. H. Preparation of Large-Area Graphene Oxide Sheets with a High Density of Carboxyl Groups Using O2/H2 Low-Damage Plasma. Surf. Coatings Technol. 2016, 303, 170–5.

[24] Zelechowska, K.; Prześniak-Welenc, M.; Łapiński, M.; Kondratowicz, I.; Miruszewski, T. Fully scalable one-pot method for the production of phosphonic graphene derivatives. Beilstein J. Nanotechnol., 2017, 8 [1], 1094–103.

[25] Kondratowicz, I.; Zelechowska, K. Graphene Oxide as Mine of Knowledge: Using Graphene Oxide to Teach Undergraduate Students Core Chemistry and Nanotechnology Concepts. J. Chem. Educ. 2017, 94 [6], 764–768.

[26] Kondratowicz, I.; Nadolska, M; Zelechowska, K.; Jazdzewska, A.; Gazda, M. Comprehensive Study on Graphene Hydrogels and Aerogels Synthesis and Their Ability of Gold Nanoparticles Adsorption. Coll Surf A, 2017, 528, 65–73.

[27] Crist, B.V. Handbook of Monochromatic XPS Spectra, Wiley, Chichester 2000

[28] Slepička, P.; Peterková, L.; Rimpelová, S.; Pinkner, A.; Slepičková Kasálková, N.; Kolská, Z.; Ruml, T.; Švorčík, V. Plasma activated perfluoroethylenepropylene for cytocompatibility enhancement, Polym. Deg. Stab. 130 (2016) 277-287

[29] Michaljaničová, I.; Slepička, P. ; Hadravová, J. ; Rimpelová, S. ; Ruml, T.; Malinský, P.; Veselý, M. and Švorčík, V. High power plasma as an efficient tool for polymethylpentene cytocompatibility enhancement, RSC Adv. 6 (2016) 76000-76010.

[30] Slepička, P.; Trostová, S.; Slepičková Kasálková N.; Kolská Z.; Malinský, P.; Macková, A.; Bačáková, L.; Švorčíka, V. Nanostructuring of polymethylpentene by plasma and heat treatment for improved biocompatibility, Polym. Deg. Stab. 97 (2012) 1075-1082

[28] King, A. A. K.; Davies, B. R.; Noorbehesht, N.; Newman, P.; Church, T. L.; Harris, A. T.; Razal, J. M.; Minett, A. I. A New Raman Metric for the Characterisation of Graphene Oxide and Its Derivatives. Sci. Rep. 2016, 6, 19491.

[29] Li, Z.; Xu, Y.; Cao, B.; Qi, L.; He, S.; Wang, C.; Zhang, J.; Wang, J.; Xu, K. Raman Spectra Investigation of the Defects of Chemical Vapor Deposited Multilayer Graphene and Modified by Oxygen Plasma Treatment. Superlattices Microstruct. 2016, 99, 125–130.

[30] Mohan, V. B.; Brown, R.; Jayaraman, K.; Bhattacharyya, D. Characterisation of Reduced Graphene Oxide: Effects of Reduction Variables on Electrical Conductivity. Mater. Sci. Eng. B Solid-State Mater. Adv. Technol. 2015, 193, 49–60.

[31] Childres, I.; Jauregui, L. a; Tian, J.; Chen, Y. P. Effect of Oxygen Plasma Etching on Graphene Studied with Raman Spectroscopy and Electronic Transport. Analysis 2010, 10.

[32] Stobinski, L.; Lesiak, B.; Malolepszy, A.; Mazurkiewicz, M.; Mierzwa, B.; Zemek, J.; Jiricek, P.; Bieloshapka, I. Graphene Oxide and Reduced Graphene Oxide Studied by the XRD, TEM and Electron Spectroscopy Methods. J. Electron Spectros. Relat. Phenomena 2014, 195, 145–154.

[33] Abulizi, A.; Okitsu, K.; Zhu, J. J.; Bo, Z.; Shuai, X.; Mao, S.; Yang, H.; Qian, J.; Chen, J. J.-T. J.; Yan, et al. Vitamin C Is an Ideal Substitute for Hydrazine in the Reduction of Graphene Oxide Suspensions. J. Phys. Chem. C 2013, 4, 6426–6432.

[34] Chen, W.; Yan, L.; Bangal, P. R. Preparation of Graphene by the Rapid and Mild Thermal Reduction of Graphene Oxide Induced by Microwaves. Carbon, 2010, 48, 1146–1152.

[35] Feng, H.; Cheng, R.; Zhao, X.; Duan, X.; Li, J. A low-temperature method to produce highly reduced graphene oxide. Nat. Commun., 2013, 4, 1537–9.

[36] Mano, N.; Edembe, L. Bilirubin oxidases in bioelectrochemistry : Features and recent findings. Biosens Bioelectron, 2013, 50, 478–485.

[37] Shleev, S.; El, A.; Ruzgas, T.; Gorton, L. Direct Heterogeneous Electron Transfer Reactions of Bilirubin Oxidase at a Spectrographic Graphite Electrode. Electrochem Commun, 2004, 6, 934–939.

[38] Zhang, C.; Chen, S.; Alvarez, P. J. J.; Chen, W. Reduced Graphene Oxide Enhances Horseradish Peroxidase Stability by Serving as Radical Scavenger and Redox Mediator. Carbon. 2015, 94, 531–538.

[39] Zhang, H.; Weber, E.J. Elucidating the role of electron shuttles in reductive transformations in anaerobic sediments, Environ. Sci. Technol. 2009, 43, 1042–48.

[40] Jiang, J.; Bauer, I.; Paul, A.; Kappler, A. Arsenic redox changes by microbially and chemically formed semiquinone radicals and hydroquinones in a humic substance model quinone, Environ. Sci. Technol. 2009, 43, 3639–45.

[41] C.-F. Ma, Q. Gao, K.-S. Xia, Z.-Y. Huang, B. Han, C.-G. Zhou, Three-dimensionally porous graphene: A high-performance adsorbent for removal of albumin-bonded bilirubin, Colloids Surf. B. 149, [2017], 146–153.

[42] B. R. Muller, Effect of particle size and surface area on the adsorption of albumin-bonded bilirubin on activated carbon, Carbon,48, [2010], 3607–15.

[43] L.Cao, R.D. Schmid, Carrier-bound Immobilized Enzymes: Principles, Application and Design. ISBN: 978-3-527-31232-0, February 2006.

[44] Shiba, S.; Inoue, J.; Kato, D.; Yoshioka, K.; Niwa, O. Graphene modified electrode for the direct electron transfer of bilirubin oxidase. Electrochem, 2015, 83[5], 332–334.

[45] Tkac, J.; Filip, J. Effective bioelectrocatalysis of bilirubin oxidase on electrochemically reduced graphene oxide. Electrochem Commun, 2014, 49, 70–74.

[46] Lalaoui, A.; Le Goff, A.; Holzinger, M.; Mermoux, M.; Cosnier, S. Wiring Laccase on Covalently Modified Graphene: Carbon Nanotube Assemblies for the Direct Bio-electrocatalytic Reduction of Oxygen. Chemistry, 2015, 21[8], 3198-201, doi: 10.1002/chem.201405557

[47] Filip, J.; Andicsov-Eckstein, A.; Vikartovska, A.; Tkac, J. Immobilization of Bilirubin Oxidase on Graphene Oxide Flakes with Different Negative Charge Density for Oxygen Reduction. The Effect of GO

Charge Density on Enzyme Coverage, Electron Transfer Rate and Current Density. Biosens. Bioelectron. 2017, 89, 384–389.

Graphical abstract
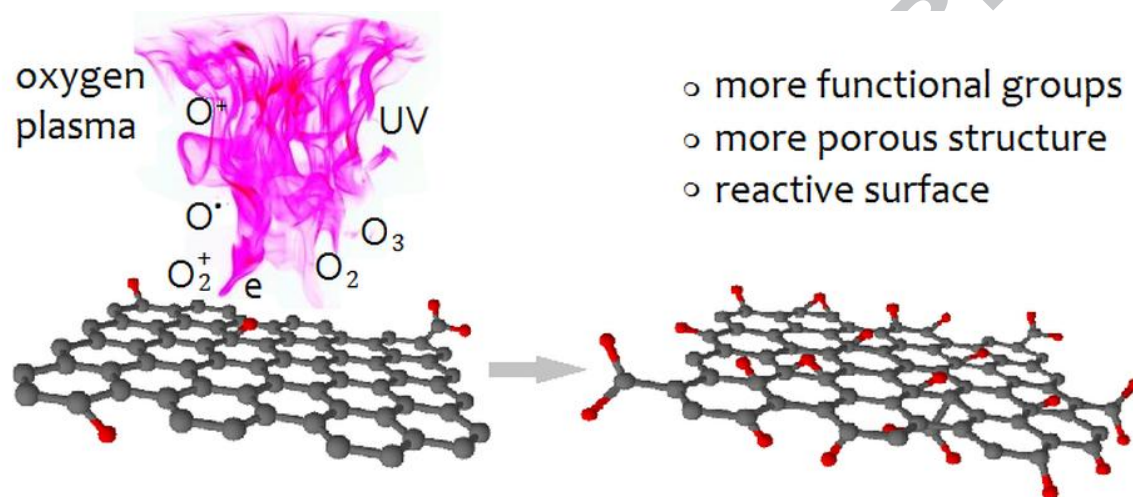
Highlights

- O_2 plasma was used for introducing oxygen-containing groups on rGO surface
- Exposure time has an influence on the amount and type of functional groups
- Porosity and surface area increased after plasma treatment
- Electrocatalytic current density was doubled for BOD-modified rGO-10min electrode
- O_2 plasma-treated rGO surface served as suitable platform for BOD adsorption